Research Square

Preprints are preliminary reports that have not undergone peer review.
They should not be considered conclusive, used to inform clinical practice,
or referenced by the media as validated information.

The importance of large trees as carbon sinks in UK woodlands

Phil Wilkes

p.wilkes@kew.org

Royal Botanic Gardens

Guilherme Castro

Royal Botanic Gardens

Mathilda Digby

Royal Botanic Gardens

Isabel Openshaw

Royal Botanic Gardens

Robert Barber

Royal Botanic Gardens

Gary Egan

Royal Botanic Gardens

Justin Moat

Royal Botanic Gardens

Rebecca Roberts

Royal Botanic Gardens

Tim Wilkinson

Royal Botanic Gardens

Research Article

Keywords: temperate woodlands, aboveground carbon, terrestrial LiDAR, allometry, United Kingdom

Posted Date: July 16th, 2026

DOI: https://doi.org/10.21203/rs.3.rs-10017170/v1

License: This work is licensed under a Creative Commons Attribution 4.0 International License.
Read Full License

Additional Declarations: No competing interests reported.

The importance of large trees as carbon sinks in UK woodlands

Phil Wilkes[1*], Guilherme Castro[1,2], Mathilda Digby[1,3], Isabel Openshaw[1], Robert Barber[1], Gary Egan[1], Justin Moat[1], Rebecca Roberts[1], Tim Wilkinson[1]

[1]Royal Botanic Gardens Kew, UK.
[2]Royal Holloway University of London, UK.
[3]University of Bristol, UK.

*Corresponding author(s). E-mail(s): p.wilkes@kew.org;

Abstract

Background: Temperate forests are globally important sinks of terrestrial carbon, therefore accurately mapping the distribution of carbon in these forests is an important first step in preserving this sink as well as to meet reporting requirements for country's progressing towards net-zero. Conventional size-to-mass methods to estimate the aboveground carbon (AGC) pool are not scale invariant and tend to underestimate the contribution of large trees. Here, we use terrestrial LiDAR to estimate AGC density across three forest and woodland types typical of the UK, and compare these to estimates derived from widely applied size-to-mass allometric approaches.

Results: Analysis of terrestrial LiDAR data captured across Kew Wakehurst, UK, indicate large trees are a disproportionate sink of AGC across both broadleaf woodland and conifer plantation. A suggested reason for this is the allocation of woody material to support the larger, spreading crowns of dominant trees which is not captured in existing allometry. A comparison with existing approaches reveals an underestimation of AGC across all three forest types, for example, the UK's Woodland Carbon Code (WCC) underestimated AGC by up to 70% in ancient broadleaf woodlands when compared to a terrestrial LiDAR approach.

Conclusion: Application of allometric methods to out-of-sample woodland types inevitably leads to an underestimation in AGC. We stress that existing methods, such as the WCC, are fit for purpose in the woodland types they are intended for; however, caution must be used when applying these methods more broadly. Owing to the concentration of AGC in a few large trees, we suggest new size-to-mass allometry needs to be developed using appropriately sized trees. As

destructive harvest of large trees is rarely feasible, terrestrial LiDAR methods could be used to estimate the "mass" side of a size-to-mass equation.

Keywords: temperate woodlands, aboveground carbon, terrestrial LiDAR, allometry, United Kingdom

1 Introduction

Globally, forests are estimated to represent a carbon (C) sink of 861 ± 66 Pg where 42% is attributed to the "live" predominantly aboveground carbon (AGC) pool [1, 2]. Within the aboveground pool, the distribution of AGC is highly skewed towards large trees where 1% of the largest individuals accounts for an estimated 90% of the sink [3]. Accurately estimating forest AGC, particularly the contribution of larger trees, is key to mapping distribution and ultimately protecting the forest C sink. However, commonly applied methods that use a tree size-to-mass ratio to estimate AGC are poorly calibrated for large trees, resulting in a likely underestimation of this cohort [4, 5].

Mapping of AGC often takes a "bottom-up" approach where the AGC of individual trees or forest patches is measured or estimated and then scaled across whole forests, regions, continents and globally with remote sensing [6–9]. Underpinning these approaches are size-to-mass allometric equations that predict AGC of a whole tree (or components there of [10]) from a more easily measured attribute, such as diameter at breast height (DBH) or tree height. To calibrate an allometric equation requires a representative set of trees to be harvested and weighed, followed by a analysis to determine wood density. However, owing to logistical, expense and ethical constraints, calibration datasets are often skewed towards a smaller cohort of trees [11] and the resulting form of an allometric equation is not necessarily transferable to larger trees [4, 12]. There are relatively few examples of destructive harvest to estimate carbon density for larger trees or large areas of forest [12]. One landmark example is that of Bunce [13], who in 1968 felled and weighed 207 individual trees across 4 sites in the Lake District, UK. The resulting allometric equations have since been applied to geographic locations, tree species and tree size distributions far beyond that of the upland forests they were intended for [4].

Over the past two decades, terrestrial LiDAR methods have been developed to generate estimates of AGC for trees in forests globally [12, 14]. Terrestrial LiDAR can generate a millimetre accurate 3D point cloud representation of a forest plot that allows mapping of tree stems, branches and leaves from the forest floor to the top of the canopy. Point clouds can then be transformed into estimates of woody volume using a Quantitative Structure Model or QSM, this encloses the point data with as a set of geometric primitives such cylinders [15], mass is then estimated by multiplying volume by an estimate of wood density [6, 16]. Importantly, terrestrial LiDAR methods are agnostic to tree size and can accurately estimate AGC across tree size distributions. Comparisons of terrestrial LiDAR and commonly applied allometric equations suggest terrestrial LiDAR to be more accurate, particularly for trees >1000 kg [12].

Temperate woodlands, such as those in the Europe and the UK, are significant sinks of carbon [17, 18]. In 2025, 3.3M ha of the UK was forested, storing an estimated 102.5 M t C [19]. Mean AGC density for UK woodlands and forest is ˜40 t C ha^{-1} [20]; maximum carbon densities are found in old-growth woodlands with an estimated AGC density of ˜65 t C ha^{-1} [21] (assuming a 46:54 "live" to soil carbon ratio, and a 70:30 shoot to root ratio [20]). However, these estimates are modelled using data derived from managed woodlands e.g. for biofuel [22], where trees <30 cm DBH that may underestimate the contribution of large trees. Calders et al. [23] estimate an AGC density of >200 t C ha^{-1} for an area of ancient woodland in Oxfordshire, UK.

In the UK, millennia of woodland management for wood, timber and agriculture has produced a diverse mosaic of managed and semi-natural woodlands [24]. UK woodland structure and composition remain dynamic, where changing management practice, competing land-use, pests and disease and climate change are altering AGC distributions [25, 26]. Once-widespread traditional silvicultural practices have since declined substantially, for example, the area of actively managed coppice woodland has decreased by 90% in less than a century [27, 28]. Concurrently, the expansion of modern conifer plantation forestry has substantially reshaped the composition of UK woodlands; since the turn of the 20^{th} Century, 40% of ecologically important and carbon-dense ancient woodland has been converted to plantation [29] and plantation now comprises ˜50% of total forest area [30]. Most recently, UK government net-zero targets [31] and carbon as a fungible commodity is changing how forests are planted and managed in the UK; since 2021 92,794 ha of new woodland has been planted under the UK Government's Woodland Carbon Code (WCC) scheme [19].

Accurately estimating AGC of UK woodlands is important for a number of reasons including national greenhouse gas inventory reporting [32], monitoring degradation and loss as a function of climate change and other pressures [19], informing management and succession planning [33]; all of which underpin the UK's progress towards net zero targets. Our hypothesis is that, across woodland types, the contribution of large trees to the total AGC pool is currently significantly underestimated. To test this hypothesis we estimate AGC using terrestrial LiDAR and commonly used inventory methods across three UK woodland types. We conclude by making recommendations for improving the representation of large trees in AGC modelling and accounting.

2 Methods

2.1 Location

This study was conducted at Kew Wakehurst, a 211 ha estate in the county of West Sussex, UK (Figure 1). The landscape comprises an historic botanic garden (˜30%) and semi-natural habitats (˜70%) representative of the High Weald National Landscape. The treescape of Kew Wakehurst is typical of southern England with a mosaic of semi-natural and managed broadleaf woodlands and conifer plantations. The woodlands of Kew Wakehurst face similar pressures and disturbances to the rest of the UK [25]. For example, the 1987 hurricane uprooted many large and mature trees across Kew Wakehurst (*pers. comm.* Iain Parkinson, Horticultural Director, Kew Wakehurst);

more recently *Hymenoscyphus fraxineus* (ash dieback) have significantly impacted *Fraxinus excelsior* (ash) tree populations.



Fig. 1: Location Kew Wakehurst and plots within the landscape. Canopy height values were generated from UK Environment Agency airborne LiDAR data [34]

2.2 Plot locations

Previous studies have estimated the AGC of Kew Wakehurst's *Sequoia giganteum* population [35] and exotic and native trees in the Living Collection [36]. For this study, three distinct forest types typical of southern UK woodlands were selected (Figure 1).

The broadleaf woodland plots are situated on the western slopes of a steep sided valley that is designated a Site of Special Scientific Interest (SSSI) [37]. Tree species and are dominated by *Quercus robur* (Pedunculate oak), *Fagus sylvatica* (Beech),

Fraxinus excelsior with a *Corylus avellana* (hazel), *Betula betulaceae* (birch) and *Sorbus aucuparia* (rowan) understorey. The woodland has a long history of management with evidence of agriculture field systems, charcoal production, *Castanea sativa* (sweet chestnut) coppicing and smaller broadleaf plantations throughout.

The coppice woodland is actively managed on a seven-year rotation in accordance with traditional practices. Tree species primarily consist of *Corylus avellana* stools interspersed with a *Quercus robur* overstorey. Large coppice stools, an irregular mosaic of coppice areas, and a well-maintained network of access and extraction rides indicate a long history of management for wood and timber [24].

The conifer plantation, a designated Plantation on Ancient Woodland Site (PAWS) [38], was planted in the mid 20$^{\text{th}}$ Century with a monoculture of Norway Spruce (*Picea abies*) in two blocks. Sparse remnant broadleaf trees remain, with an open understorey.

For both the coppice and the conifer sites, the whole block was considered a plot (Figure 1). Plot dimensions were determined by tracing a polygon around these areas in QGIS [39] where airborne LiDAR [34] derived canopy height was used to determine extent. Owing to the greater areal extent of the broadleaf woodland, eight 40 m x 40 m (0.16 ha) subplots were identified that covered a range of stand age and species distributions (Figure 1). Once plots had been scanned with terrestrial LiDAR, accurate plot dimensions were determined by fitting a rotated rectangle around the scan positions.

2.3 Terrestrial LiDAR

Data were captured with a RIEGL VZ-400i (Horn, Austria) terrestrial LiDAR following the recommendations of [14]. Scans were acquired in an upright position only with a scan rate of 1200 KHz [40] and an angular step of 0.04 degrees. Distance between scans ranged from 10 – 20 m (Table 1) [4, 14].

Table 1: Scan characteristics by habitat type.

Habitat	Date	Area scanned (ha)	Scans ha^{-1}	Mean distance between scan positions (m)
Broadleaf	January 2023	5.1	31	19.3 (5.8)
Conifer	December 2022	0.7	128	10.7 (4.1)
Coppice	January 2023	1.3	109	12.7 (4.0)

Scans were post-processed using RiSCAN Pro (version 2.17) to co-register all scans into a common arbitrary coordinate system. The RiSCAN Pro software tools *Automatic Registration 2* and *Multi Station Adjustment* were used to generate a coarse and fine scale registration respectively. Once registered, the *riscan2ply.py* Python tool [41] were used to reproject the data into the British National Gird coordinate system (EPSG:27700), filter points by reflectance (-20 - +5 dB) and deviation (<15) and horizontally grid the point cloud into 10 m x 10 m voxels. Tiles were then processed with the *TLS2trees* pipeline [42] that performs a semantic and instance segmentation to isolate individual trees from the global point cloud. Only trees where the germination point was within the plot were processed further.

To estimate woody volume, segmented tree point clouds were processed with TreeQSM (version 2.3.1, [43]) in a two step process. First, for each tree, a sparse parameter space of the TreeQSM variables *PatchDiam1*, *PatchDiam2Min* and *PatchDiam2Max* were iterated over to generate initial estimates of optimal parameter values. As TreeQSM is stochastic, for each parameter combination a set of 5 models was produced, resulting in a maximum of 125 parameter combinations and 625 QSM models per tree. The optimal per tree parameter set was then chosen using the lowest mean cylinder-to-point distance. Secondly, a further 100 models were generated using the optimal parameter set, from which mean total volume V and standard deviation σ_V were derived. Distributions of V were found to be approximately Normal and therefore the standard deviation calculation was valid.

To convert V to mass, a species specific mean wood density value ρ was taken from the Global Wood Density Database [44]. As there are limited samples for each species (mean = 2.2 samples), wood density standard deviations σ_ρ were calculated at Family level where samples were constrained to the Europe Region where possible (Table 2). A biome specific biomass to carbon ratio CF of 0.488 and 0.508 for temperate angiosperms and conifers respectively was used [45]. A 95% confidence interval of 0.006 was given for both temperate angiosperms and conifers CF [45], this was converted to standard deviation $\sigma_{\text{CF}} = (0.006/1.96)$ / CF.

Table 2: Mean and standard deviation wood density values taken from [44]. *mean value derived from samples outside of Europe.

		wood density		
Family	Species	count	mean	std
Aquifoliaceae	*Ilex aquifolium**	1	0.65	-
Betulaceae	*Betula pendula*, *Corylus avellana*, *Alnus glutinosa*	7	0.55	0.11
Fagaceae	*Fagus sylvatica*, *Quercus robur*, *Quercus petraea*, *Castanea sativa**	12	0.61	0.14
Malvaceae	*Tilia cordata*	3	0.44	0.04
Oleaceae	*Fraxinus excelsior*	3	0.64	0.14
Pinaceae	*Picea abies*, *Pinus sylvestris*	17	0.43	0.06
Rosaceae	*Prunus avium*, *Malus sylvestris*, *Sorbus aucuparia*	8	0.60	0.06
Salicaceae	*Salix caprea*	6	0.37	0.05
Sapindaceae	*Acer pseudoplatanus*, *Acer campestre*	6	0.51	0.01
Taxaceae	*Taxus baccata*	2	0.55	-

AGC and associated uncertainty σ_{AGC} (both in tonnes) was calculated for each tree i using the following

$$\text{AGC}_i = V_i \cdot \rho_i \cdot \text{CF}_i \tag{1}$$

$$\sigma_{\text{AGC}_i} = |\text{AGC}_i| \cdot \sqrt{\left(\frac{\sigma_{\text{V}_i}}{\text{V}_i}\right)^2 + \left(\frac{\sigma_{\rho_S}}{\rho_S}\right)^2 + \left(\frac{\sigma_{\text{CF}_S}}{\text{CF}_S}\right)^2} \tag{2}$$

where S are species specific values.

Total habitat AGC_H and associated uncertainty σ_{AHC_H} was then calculate using Equations 3 and 4. To estimate habitat level uncertainty, an assumption was made that errors are independent between trees [16].

$$\mathrm{AGC}_H = \sum_{i=1}^{n} \mathrm{AGC}_i \tag{3}$$

$$\sigma_{\mathrm{AGC}_H} = \sqrt{\sum_{i=1}^{n} {\sigma_{AGC_i}}^2} \tag{4}$$

Finally, to determine AGC density $\mathrm{AGC}_H\ \mathrm{ha}^{-1}$ and uncertainty $\sigma_{\mathrm{AGC\ ha^{-1}}}$ the following equations were used:

$$\mathrm{AGC}_H\ \mathrm{ha}^{-1} = \mathrm{AGC}_H / A_H \tag{5}$$

$$\sigma_{\mathrm{AGC\ ha^{-1}}} = |\mathrm{AGC}_H| \cdot \sqrt{\left(\frac{\sigma_{\mathrm{AGC}_H}}{\mathrm{AGC}_H}\right)^2 + \left(\frac{\sigma_A}{A}\right)^2} \tag{6}$$

where A is total plot area. Standard deviation for area σ_A was estimated by jittering the vertices of the boundary points in 2D using a normal distribution ($\sigma = 1$ m, $N = 100$).

2.4 Inventory measurements and allometry

To compare terrestrial LiDAR derived AGC with commonly applied allometric approaches, a subset of larger trees were inventoried where species and DBH were recorded. A map derived from terrestrial LiDAR was used to locate trees in plots and directly link a measured tree with its digital counterpart.

For broadleaf species, AGC was estimated using the Bunce "Combined" equation [13]. Conifers were dominated by *Picea abies* therefore the equation of Černý [46] was used, taken from [10], as this mostly closely matched tree size distributions. AGC density were also computed for all woodland types using the UK's Woodland Carbon Code (WCC) method [47].

All methods require DBH as an input variable. As not all trees were inventoried, two estimates were derived (1) using only manually measured DBH, and (2) where DBH values were derived from TreeQSM; a Bland-Altman test indicates that QSM estimated DBH overestimates manually measured DBH by ˜1% (see Supplementary Material). However, it was noted that for multi-stemmed trees TreeQSM tended to enclose all stems in a single cylinder (e.g. *Corylus avellana* coppice stools) , for this reason when using TreeQSM estimate DBH, *Corylus avellana* were excluded. The WCC methods for conifers require an estimate of tree height, here this was derived from segmented terrestrial LiDAR point clouds. For broadleaf species, the WCC requires an estimate of timber height defined as the distance from the ground to the "spring of the crown" i.e. the lowest point at which no main stem is distinguishable [48]. "Spring of the crown" was estimated for each tree from the QSM as the lowest point at which a child branch has the same diameter (±10%) as the primary stem. A workflow for

Woodland Carbon Code methods are presented in the Supplementary Material. All methods return estimates of aboveground biomass, these were converted to AGC by multiplying with the tree type specific CF (see above).

It is acknowledged that none of these equations were derived specifically for Kew Wakehurst or woodlands that could be described as similar e.g. none were derived for ancient or coppice woodland. However, in the absence of species or location specific allometric equations these are likely candidate approaches for estimating AGC.

3 Results

3.1 AGC estimates for individual trees

Broadleaf trees are the largest sinks of AGC across all forest types in this study (Figure 2). The largest individual tree by AGC is a *Quercus robur* containing 13.9 ± 3.46 (1 s.d.) t C followed by a *Fagus sylvatica* with an estimated 13.6 ± 3.22 t C (Table 3 and Figure 2). Across all three habitats, per tree contribution to habitat level AGC density is significantly skewed towards larger individuals (Figure 3). For example, for the broadleaf and coppice plots, 50% of AGC is in the largest 3% of trees (13 trees ha^{-1}) and 4% of trees (16 trees ha^{-1}) respectively. Even for the relatively even aged conifer plantation ˜50% of AGC is in ˜25% of the largest trees. It is acknowledged that these percentile thresholds are determined by an arbitrary DBH threshold (0.1 m); however, we suggest this estimate is conservative compared to [3] who used a DBH threshold of 0.01 m.



Fig. 2: Point cloud representations of segmented trees for broadleaf (top) coppice (middle) and conifer plots (bottom). The value above each tree is the estimated AGC in tonnes.

Individual tree level uncertainty is greatest in the broadleaf and coppiced plots where, considering all trees, mean AGC standard deviation is 41% and 33% respectively. However, when considering the largest trees that comprise 90% of AGC per

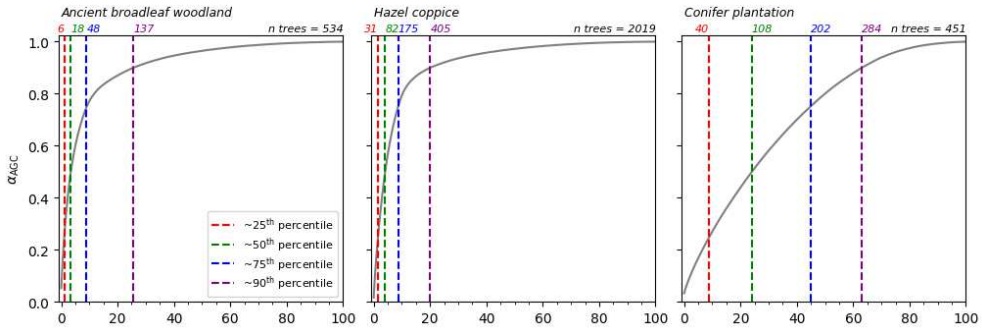


Fig. 3: Per tree relative contribution to plot level AGC. The values along the top axes are the number of trees for the corresponding percentage contribution.

Table 3: Individual trees measurements derived from point clouds and QSM. * *Corylus avellana* removed owing to poor DBH estimation of multistem trees with QSM

	height [m]			DBH [m]*			crown area [m^2]			AGC [t]		
habitat	mn	std	max	mn	std	max	mn	std	max	mn	std	max
broadleaf	10.4	7.8	37.9	0.38	0.29	1.41	55.2	89.8	767.0	0.48	1.39	13.63
coppice	8.0	6.4	29.5	0.62	0.25	1.40	44.5	84.1	810.5	0.42	1.15	13.92
conifer	19.6	8.0	28.9	0.32	0.12	0.99	32.9	23.6	273.4	0.25	0.24	3.75

habitat, uncertainty reduces to ˜27% in both the broadleaf and coppice habitats (Figure 4A). For conifer trees, AGC uncertainty is 18%, significantly lower than for broadleaf trees. Two suggested reasons for this are (1) *Picea* species have a simpler architecture compared to broadleaf trees and (2) the conifer plot has a sparser understorey that reduces occlusion. Contribution to uncertainty from the terms in Equation 1 are illustrated in Figure 4B-C. For smaller trees, uncertainty in woody volume is the predominant source whereas for larger trees wood density is the largest source (70-80%, Figure 4C); for the largest 10 trees captured, mean uncertainty from wood density comprised >90%. The contribution to uncertainty of CF is <1% and is therefore not illustrated.

3.2 Habitat level AGC estimates

AGC density ranges from 130.2 t C ha^{-1} for the conifer plantation to 218.9 t C ha^{-1} for broadleaf woodland (Table 4). Comparing the broadleaf and coppice woodlands, stem density (Table 4) and tree height and projected crown area (Table 3) are greater in the broadleaf woodland that has as led to higher AGC density in the former. Smaller uncertainty estimates for coppice woodland compared with broadleaf woodland is due to the much larger plot size for the former.

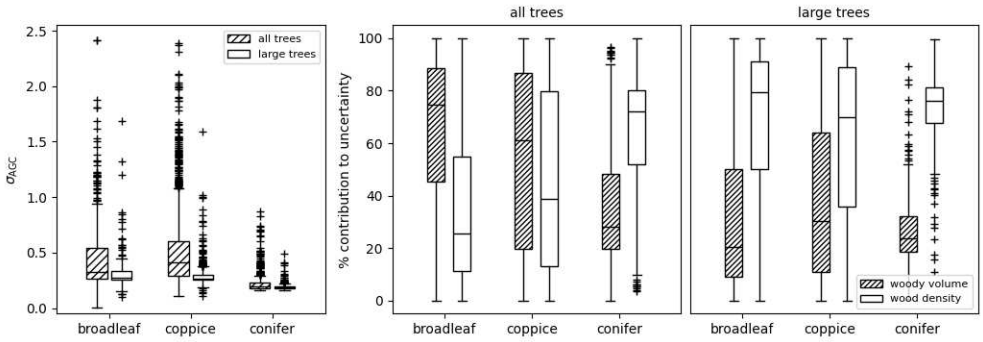


Fig. 4: Per tree AGC uncertainty estimates comparing all trees and "large" trees that comprise 90% of total AGC. [left] shows individual tree σ_{AGC} by habitat, [centre] and [right] illustrate contribution to uncertainty from woody volume and wood density from "all" and "large" trees.

Across three forest types (total area 7.3 ha) a total of 2,481 trees were segmented from terrestrial LiDAR point clouds that met the criteria of within plot germination and estimated DBH > 0.1 m. A further 2,108 trees were segmented but excluded as they had an estimated DBH < 0.1 m. It is evident from Figure 2 that instance segmentation suffered from commission and omission errors e.g. portions of neighbouring crowns are segmented together. However, [42] reported minimal woody volume bias when comparing *TLS2trees* output with manually segmented tree point clouds in a similar UK woodland.

Table 4: Habitat level tree and AGC density

	stems		Plot area [ha]		AGC [t]		
habitat	N	ha^{-1}	ha	std	$\sum$	ha^{-1}	$\sigma_{\mathrm{AGC\ ha^{-1}}}$
broadleaf	468	371	1.26	0.20	263.8	209.3	34.50
coppice	1573	308	5.10	0.15	841.8	165.1	5.57
conifer	439	510	0.86	0.10	112.6	130.1	15.06

3.3 A comparison with allometric derived values of AGC

Terrestrial LiDAR derived AGC values for broadleaf trees and habitats are consistently higher than estimated by the Bunce "Combined" equation (Figure 5 and Table 5). Figure 5A illustrates that overestimation of AGC is evident across all tree sizes. Residual error between methods identifies a systematic bias that increases with tree size (Figure 5B). Summing AGC values for the broadleaf and coppice woodlands reveals terrestrial LiDAR derived estimates are between 50% and 60% greater than allometric estimates respectively. For *Picea abies*, terrestrial LiDAR derived and allometry

values are generally in good agreement (Figure 5A) across tree size; summed AGC indicates an underestimation by 10%-20% by terrestrial LiDAR.

A comparison with Woodland Carbon Code (WCC) derived values indicates a significant difference between methods across all three forest types (Table 4). In the broadleaf and coppice plots, WCC values are approximately 30% and 50% that predicted by terrestrial LiDAR and Bunce allometry respectively. A suggested reason for this is the underestimation of crown mass i.e. the mass of timber above the "spring of the crown". Using the the broadleaf habitat as an example and following the method presented in Appendix 5 of [47], the WCC method estimates total crown C mass to be 20.9 tonnes; this compares to 157.3 tonnes using TreeQSM derived values.

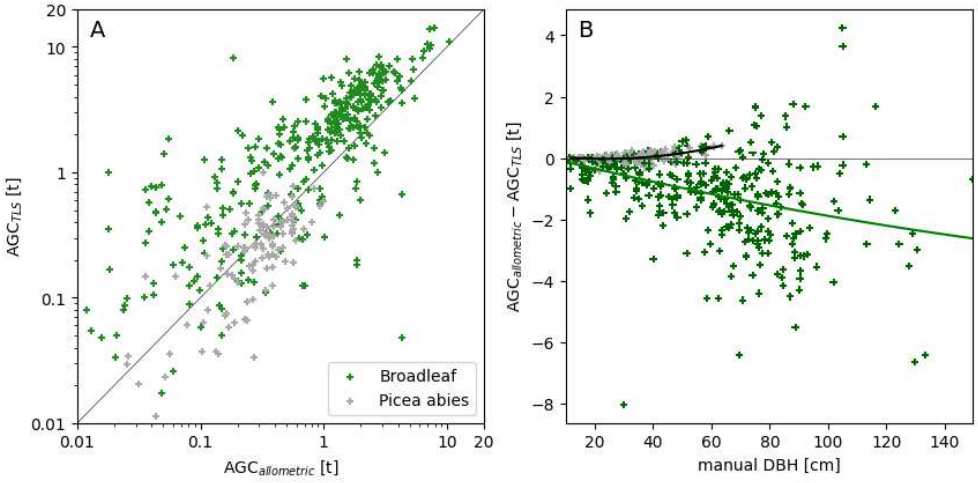


Fig. 5: A comparison of terrestrial LiDAR and allometry derived AGC values for broadleaf and coppice species where (A) illustrates the systematic difference between methods and (B) displays the residual difference between methods including a non-linear regression line.

4 Discussion

Analysis of terrestrial LiDAR data reveals that in the woodlands of Kew Wakehurst, a small cohort of large broadleaf trees represent the majority sink of aboveground carbon (AGC). Although a similar trend has also been observed for a *Acer pseudoplatanus* dominated ancient woodland in the UK [4], as well as globally [3, 49], here we identify the importance of large trees across a range of woodland types common to the UK.

Large trees are a common feature of semi-natural and managed woodlands in the UK e.g. as remanent coppice stools, wood pasture or boundary trees [24, 50]. The largest individual trees in this study are situated on the edge of a field system that has since reverted to secondary woodland or are situated in the managed coppice woodland. Their large size is a result of woodland management practice where a cycle

Table 5: A comparison of terrestrial LiDAR (TLS), allometry and Woodland Carbon Code (WCC) estimates of AGC. *Inventoried subset* uses manual measurement of DBH as the variable in the allometric and WCC estimation, whereas *all trees* uses DBH estimated by TreeQSM. *All trees* also excludes *Corylus avellana*, see Section 2.4.

	inventoried subset (t ha^{-1})				*all trees** (t ha^{-1})			
habitat	N	TLS	allometry	WCC	N	TLS	allometry	WCC
broadleaf	82	101.5	67.1	30.3	173	173.5	107.0	47.1
coppice	286	139.1	83.2	41.2	438	141.2	88.0	41.4
conifer	118	43.0	47.7	28.9	291	130.8	159.4	93.7

of agricultural abandonment has likely resulted in trees that were originally open-grown (i.e. managed and with less competition) becoming incorporated into secondary or managed woodland. Large trees are often associated with other significant pools of carbon, including root biomass and elevated soil organic carbon in the surrounding rhizosphere[20, 51, 52] as well as other important habitat and cultural features [53]. Therefore, woodland management strategies, supported by appropriate policy, should prioritise the retention of large trees, as well as the recruitment of future large individuals, to ensure these habitats remain significant carbon sinks [54].

The commonly used allometric equations tested here are not scale invariant [4] and therefore applying equations to trees that are out of sample will inevitably lead to errors [11]. As shown here, and by others [4, 12, 55], commonly applied allometric equations tend to underestimate AGC of large trees as large trees are under-represented (or missing) in training data. For example, the DBH range used to create the Bunce equation does not overlap with the DBH range of the trees that account for 90% of measured AGC (Figure 6). Equations for predicting others pools of carbon e.g. root biomass, that rely on size-to-mass relationships are therefore also likely to underestimate the contribution of large trees, leading to even larger discrepancies of gross habitat carbon density. Making the assumption that AGC for all large trees inside and outside woodlands [56] are underestimated would have significant implications on the value attributed to these trees, and the statutory reporting that size-to-mass relationships underpin.

A suggested reason for the unsuitability of existing allometry is a shift in AGC allocation to a tree's crown with increasing size [55] i.e. large diameter branches are required to support a larger spreading crown (Figure 6). As shown in Figure 6, the mean ratio shifts from 45:55 (stem:crown) in trees where DBH $<$30 cm to 29:71 in trees where DBH $\geq$ 30 cm, a Welch's t-test indicates there is a statistically significant difference in C allocation between these two cohorts ($t=17.71$, $p<0.001$). For this reason, projected crown area has been shown to be a good predictor of AGC of large and open-grown trees [4, 14, 55].

If current allometry is not suitable for large trees then how can we predict their mass? It is important to remember that any method does not necessarily need to be precise for an individual tree but does need to be accurate for the woodland population (be it local, national or global). Residual variance may increase for larger trees owing

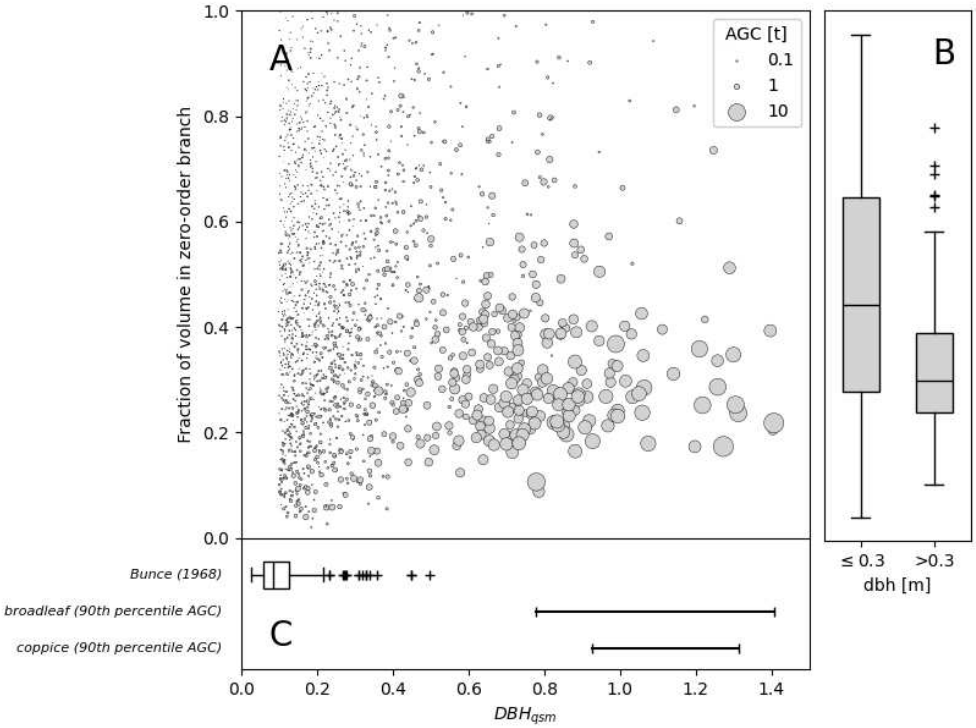


Fig. 6: The ratio of stem to total AGC illustrating the partitioning of AGC between stem and crown as a function of tree size. [**A**] a scatter plot of all broadleaf trees where DBH >0.1 m, point size is determined by total AGC, [**B**] compares the distribution of ratios between trees where DBH is below or greater than 0.3 m, and [**C**] compares the DBH distribution used to construct Bunce (taken from [23]) to that of the trees that comprise 90% of habitat level AGC, highlighting the disparity between the groups. Stem AGC is calculated from each QSM by summing AGC of cylinders labelled as *branch 0*.

to greater heterogeneity in crown architecture associated with location, ontogeny and senescence; however, as long as new equations show no systematic bias they should be considered suitable. To derive a new allometric equation suitable for large trees would require sufficient sampling, across species and location, to capture variability in tree mass and crown shape. As destructive campaigns for large trees are unlikely to yield a large enough sample (see Introduction), a terrestrial LiDAR could be used to derive an estimate of AGC. However, terrestrial LiDAR can often poorly estimate other structural traits such as DBH; therefore a hybrid approach, that couples terrestrial LiDAR with in-situ measurements of a predictor variable such as manually measured DBH. Examples of such efforts in the tropics include ForestScan [57] and GEO-TREES (https://www.geo-trees.org/). However, this would not address the current limited number of wood density measurements (Table 2) that are required when converting

from volume to mass and are a significant source of uncertainty (Figure 4). Therefore we also suggest a concerted effort would be required to develop a database of wood density samples from larger trees e.g. using increment borers.

5 Conclusion

Previous research has identified that the underestimation of AGC in large trees compounds to a significant underestimation of the total woodland carbon pool. This study extends these findings to other semi-natural and managed woodlands in the UK and therefore implies the potential for a gross underestimation in reported national level AGC values. Here we show that a majority fraction of AGC is concentrated in a few large trees and that this cohort are poorly characterised by existing allometry, principally owing to the underestimation of AGC in tree crowns. It is strongly emphasised that we are not suggesting existing allometric methods are unsuitable for estimating AGC in UK woodlands they were intended for; however, we do suggest that caution is required when applying these allometric methods to out-of-sample trees i.e. in woodlands where there are larger trees. We are also not suggesting that size-to-mass methods are unsuitable for large trees; however, we do recommend that new allometries for estimating AGC of UK woodlands are constructed with the knowledge of the importance of larger trees as carbon sinks as well as the morphological differences between smaller and larger trees. As the felling of large, usually older and more ecologically valuable, trees is undesirable and increasingly difficult at scale, we suggest that terrestrial LiDAR methods could be used to estimate the "mass" component of a size-to-mass equation. Conventional inventory techniques, such as DBH measurements or remote sensing, could then still be used to operationalise these methods at scales required for national level reporting. Further, given that a substantial proportion of AGC is concentrated in a small number of large trees, woodland management, guided by appropriate policy, should prioritise their retention, alongside the recruitment of future large individuals, to maintain these habitats as significant carbon sinks.

6 Declarations

6.1 Availability of data and materials

Segmented tree point clouds, Quantitative Structure Models, a table of per tree measurements and modelled values and Python code (as Jupyter notebooks) is available from https://doi.org/10.5281/zenodo.20664592

6.2 Competing interests

The authors declare no competing interests

6.3 Funding

This research is part of the Nature Unlocked programme at Royal Botanic Gardens, Kew, funded under the Nature Returns programme, within the UK government's Shared Outcomes Fund funded by HM Treasury and co-sponsored by DEFRA and

DESNZ. Nature Returns is in partnership with Natural England, Environment Agency, Forestry Commission, University of Sussex and local partners.

6.4 Authors' contributions

PW Data Curation, Formal Analysis, Investigation, Methodology, Software, Supervision, Visualization, Writing – Original Draft Preparation. **GC** Data Curation, Formal Analysis, Investigation, Methodology, Writing – Review & Editing. **MD** Data Curation, Formal Analysis, Investigation, Methodology, Writing – Review & Editing. **IO** Formal Analysis, Methodology, Software, Writing – Review & Editing. **RB** Data Curation, Formal Analysis, Writing – Review & Editing. **GE** Investigation, Writing – Review & Editing. **JM** Conceptualization, Funding Acquisition, Methodology, Project Administration, Supervision, Writing – Review & Editing. **RR** Project Administration, Writing – Review & Editing. **TW** Investigation, Methodology, Writing – Review & Editing.

6.5 Acknowledgements

The authors would like to thank the Kew Wakehurst Horticulture team for assisting with field work.

References

[1] Pan, Y., Birdsey, R.A., Fang, J., Houghton, R., Kauppi, P.E., Kurz, W.A., Phillips, O.L., Shvidenko, A., Lewis, S.L., Canadell, J.G., *et al.*: A large and persistent carbon sink in the world's forests. Science **333**(6045), 988–993 (2011) https://doi.org/10.1126/science.1201609

[2] Bar-On, Y.M., Phillips, R., Milo, R.: The biomass distribution on Earth. Proceedings of the National Academy of Sciences **115**(25), 6506–6511 (2018) https://doi.org/10.1073/pnas.1711842115

[3] Lutz, J.A., Furniss, T.J., Johnson, D.J., Davies, S.J., Allen, D., Alonso, A., Anderson-Teixeira, K.J., Andrade, A., Baltzer, J., Becker, K.M.L., *et al.*: Global importance of large-diameter trees. Global Ecology and Biogeography **27**(7), 849–864 (2018) https://doi.org/10.1111/geb.12747

[4] Calders, K., Verbeeck, H., Burt, A., Origo, N., Nightingale, J., Malhi, Y., Wilkes, P., Raumonen, P., Bunce, R.G.H., Disney, M.: Laser scanning reveals potential underestimation of biomass carbon in temperate forest. Ecological Solutions and Evidence **3**(4), 12197 (2022) https://doi.org/10.1002/2688-8319.12197

[5] Zhou, X., Yang, M., Liu, Z., Li, P., Xie, B., Peng, C.: Dynamic allometric scaling of tree biomass and size. Nature Plants **7**(1), 42–49 (2021) https://doi.org/10.1038/s41477-020-00815-8

[6] Disney, M.I., Boni Vicari, M., Burt, A., Calders, K., Lewis, S.L., Raumonen, P., Wilkes, P.: Weighing trees with lasers: Advances, challenges and opportunities. Interface Focus **8**(2), 20170048 (2018) https://doi.org/10.1098/rsfs.2017.0048

[7] Saatchi, S.S., Harris, N.L., Brown, S., Lefsky, M., Mitchard, E.T.A., Salas, W., Zutta, B.R., Buermann, W., Lewis, S.L., Hagen, S., Petrova, S., White, L., Silman, M., Morel, A.: Benchmark map of forest carbon stocks in tropical regions across three continents. Proceedings of the National Academy of Sciences **108**(24), 9899–9904 (2011) https://doi.org/10.1073/pnas.1019576108

[8] Vorster, A.G., Evangelista, P.H., Stovall, A.E.L., Ex, S.: Variability and uncertainty in forest biomass estimates from the tree to landscape scale: The role of allometric equations. Carbon Balance and Management **15**(1), 8 (2020) https://doi.org/10.1186/s13021-020-00143-6

[9] Dubayah, R., Armston, J., Healey, S.P., Bruening, J.M., Patterson, P.L., Kellner, J.R., Duncanson, L., Saarela, S., Ståhl, G., Yang, Z., Tang, H., Blair, J.B., Fatoyinbo, L., Goetz, S., Hancock, S., Hansen, M., Hofton, M., Hurtt, G., Luthcke, S.: GEDI launches a new era of biomass inference from space. Environmental Research Letters **17**(9), 095001 (2022) https://doi.org/10.1088/1748-9326/ac8694

[10] Zianis, D., Muukkonen, P., Mäkipää, R., Mencuccini, M.: Biomass and stem volume equations for tree species in Europe. Silva Fennica Monographs **4**, 1–63 (2005) https://doi.org/10.14214/sf.sfm4

[11] Burt, A., Calders, K., Cuni-Sanchez, A., Gómez-Dans, J., Lewis, P., Lewis, S.L., Malhi, Y., Phillips, O.L., Disney, M.: Assessment of bias in pan-tropical biomass predictions. Frontiers in Forests and Global Change **3**, 12 (2020) https://doi.org/10.3389/ffgc.2020.00012

[12] Demol, M., Verbeeck, H., Gielen, B., Armston, J., Burt, A., Disney, M., Duncanson, L., Hackenberg, J., Kükenbrink, D., Lau, A., *et al.*: Estimating forest above-ground biomass with terrestrial laser scanning: Current status and future directions. Methods in Ecology and Evolution **13**(8), 1628–1639 (2022) https://doi.org/10.1111/2041-210X.13906

[13] Bunce, R.G.H.: Biomass and production of trees in a mixed deciduous woodland: I. girth and height as parameters for the estimation of tree dry weight. The Journal of Ecology **56**(3), 759–775 (1968) https://doi.org/10.2307/2258105

[14] Wilkes, P., Lau, A., Disney, M., Calders, K., Burt, A., de Tanago, J.G., Bartholomeus, H., Brede, B., Herold, M.: Data acquisition considerations for terrestrial laser scanning of forest plots. Remote Sensing of Environment **196**, 140–153 (2017) https://doi.org/10.1016/j.rse.2017.04.030

[15] Raumonen, P., Kaasalainen, M., Åkerblom, M., Kaasalainen, S., Kaartinen, H.,

Vastaranta, M., Holopainen, M., Disney, M., Lewis, P.: Fast automatic precision tree models from terrestrial laser scanner data. Remote Sensing **5**(2), 491–520 (2013) https://doi.org/10.3390/rs5020491

[16] Calders, K., Newnham, G., Burt, A., Murphy, S., Raumonen, P., Herold, M., Culvenor, D., Avitabile, V., Disney, M., Armston, J., *et al.*: Nondestructive estimates of above-ground biomass using terrestrial laser scanning. Methods in Ecology and Evolution **6**(2), 198–208 (2015) https://doi.org/10.1111/2041-210X.12301

[17] Food and Agriculture Organization of the United Nations: Global Forest Resources Assessment 2020. Technical report, FAO (2020). https://doi.org/10.4060/ca9825en . http://www.fao.org/documents/card/en/c/ca9825en

[18] Food and Agriculture Organization of the United Nations: Global forest resources assessment 2020: United Kingdom of Great Britain and Northern Ireland — country report. Technical report, FAO, Rome, Italy (2020). FAO Forestry Paper. https://openknowledge.fao.org/server/api/core/bitstreams/b4d28ddc-eb72-442c-8ce9-c0cd88608bbf/content

[19] Forest Research: Forestry statistics 2025 – chapter 4: Carbon. Technical report, Forest Research (2025). Accessed: 2025-11-26. https://www.forestresearch.gov.uk/tools-and-resources/statistics/publications/forestry-statistics/forestry-statistics-2025/2025-4-carbon/

[20] Morison, J., Matthews, R., Miller, G., Perks, M., Randle, T., Vanguelova, E., White, M., Yamulki, S.: Understanding the carbon and greenhouse gas balance of forests in Britain. Research report, Forestry Commission, Edinburgh (2012)

[21] Broadmeadow, M., Matthews, R.: Forests, carbon and climate change: the UK contribution. Technical Report FCIN048, Forestry Commission, Edinburgh, UK (June 2003). Information Note. https://www.forestresearch.gov.uk/publications/archive-forests-carbon-and-climate-change-the-uk-contribution/

[22] McKay, H.M., Hudson, J.B., Hudson, R.J.: Woodfuel resource in Britain. Final Report FES B/W3/00787/REP/1, Forestry Contracting Association, Lairg, UK (2003). DTI Publication URN 03/1436

[23] Calders, K., Verbeeck, H., Burt, A., Origo, N., Nightingale, J., Malhi, Y., Wilkes, P., Raumonen, P., Bunce, R., Disney, M.: Terrestrial laser scanning data Wytham Woods: individual trees and quantitative structure models (QSMs). Zenodo. Version 1.0 (2022). https://doi.org/10.5281/zenodo.7307956 . https://doi.org/10.5281/zenodo.7307956

[24] Rackham, O.: Trees and Woodland in the British Landscape. J. M. Dent & Sons, London (1976)

[25] Smart, S.M., Walker, C., Sier, A.R.J., Seaton, F., Kirby, K.J., Wood, C.M.: Fifty

years of change across British broadleaved woodlands: a resurvey and analysis of the “Bunce” sites 1971–’01–’21 (2024)

[26] Kirby, K.J., Bazely, D.R., Goldberg, E.A., Hall, J.E., Isted, R., Perry, S.C., Thomas, R.C.: Changes in the tree and shrub layer of Wytham Woods (Southern England) 1974–2012: Local and national trends compared. Forestry: An International Journal of Forest Research **87**(5), 663–673 (2014) https://doi.org/10.1093/forestry/cpu026

[27] Harmer, R., Howe, J.: The Silviculture and Management of Coppice Woodlands, p. 88. Forestry Commission, Edinburgh (2003)

[28] National Coppice Federation: NCFED Coppice Map. https://ncfed.org.uk/ncfed-coppice-map/. Accessed: 2025-12-10

[29] Department for Environment, Food & Rural Affairs, Forestry Commission, Natural England: Keepers of Time: Ancient and Native Woodland and Trees Policy in England. https://www.gov.uk/government/publications/keepers-of-time-ancient-and-native-woodland-and-trees-policy-in-england. Accessed: 2025-12-10 (2022)

[30] Forest Research: Forestry statistics 2025: Chapter 1 – woodland area & planting. Accredited Official Statistics Chapter 1, Forest Research, The Research Agency of the Forestry Commission, Northern Research Station, Roslin, Midlothian, EH25 9SY, United Kingdom (2025). https://cdn.forestresearch.gov.uk/2025/09/FS2025_Ch1-68d4f71b97f6f.pdf

[31] GOV.UK: 3. Reducing Emissions across the Economy. https://www.gov.uk/government/publications/net-zero-strategy/3-reducing-emissions-across-the-economy. Accessed: 2026-02-24 (2022)

[32] Department for Energy Security and Net Zero: UK greenhouse gas inventory, 1990 to 2022: Annual national inventory report. Technical report, National Atmospheric Emissions Inventory (NAEI), London, UK (2024). https://naei.energysecurity.gov.uk/greenhouse-gases/greenhouse-gas-emissions-data

[33] Forestry Commission: The UK forestry standard: The government’s approach to sustainable forestry. Technical report, Forestry Commission (2023). https://assets.publishing.service.gov.uk/media/651670336a423b0014f4c5c0/Revised_UK_Forestry_Standard_-_effective_October_2024.pdf

[34] Environment Agency: National LiDAR Programme Point Clouds. Environment Agency. Accessed: 12 January 2025. Licensed under the Open Government Licence v3.0 (2021)

[35] Holland, R., Castro, G., Chavana-Bryant, C., Levy, R., Moat, J., Robson, T., Wilkinson, T., Wilkes, P., Yang, W., Disney, M.: Giant sequoia (*Sequoiadendron*

giganteum) in the UK: Carbon storage potential and growth rates. Royal Society Open Science **11**(3), 230603 (2024) https://doi.org/10.1098/rsos.230603

[36] Revill-Hivet, E., Garfoot, L., Wilkes, P.: Estimating the aboveground biomass of Wakehurst's living collection. Technical report, Royal Botanic Gardens, Kew Wakehurst (2026). https://kew.iro.bl.uk/downloads/862a63e4-eea5-40e9-8aec-5718e9ba519e

[37] Natural England: Wakehurst and Chiddingly Woods Site of Special Scientific Interest Citation. https://designatedsites.naturalengland.org.uk/PDFsForWeb/Citation/1001409.pdf. Accessed: 2025-04-11 (1987)

[38] Natural England: Ancient Woodland (England). https://naturalengland-defra.opendata.arcgis.com/datasets/Defra::ancient-woodland-england/about. Accessed: 2025-04-11 (2023)

[39] QGIS Development Team: QGIS Geographic Information System (2023). https://www.qgis.org

[40] Verhelst, T.E., Calders, K., Burt, A., Demol, M., D'hont, B., Nightingale, J., Terryn, L., Verbeeck, H.: Implications of pulse frequency in terrestrial laser scanning on forest point cloud quality and individual tree structural metrics. Remote Sensing **16**(23), 4560 (2024) https://doi.org/10.3390/rs16234560

[41] Wilkes, P., Yang, W.: tls-tools-ucl/rxp-pipeline: rxp-pipeline. Zenodo. v0.1 (2025). https://doi.org/10.5281/zenodo.15196452 . https://doi.org/10.5281/zenodo.15196452

[42] Wilkes, P., Disney, M., Armston, J., Bartholomeus, H., Bentley, L., Brede, B., Burt, A., Calders, K., Chavana-Bryant, C., Clewley, D., *et al.*: TLS2trees: a scalable tree segmentation pipeline for TLS data. Methods in Ecology and Evolution **14**(12), 3083–3099 (2023) https://doi.org/10.1111/2041-210X.14233

[43] Raumonen, P.: InverseTampere/TreeQSM: Version 2.3.1. Zenodo. v2.3.1 (2019). https://doi.org/10.5281/zenodo.3482908 . https://doi.org/10.5281/zenodo.3482908

[44] Zanne, A.E., Lopez-Gonzalez, G., Coomes, D.A., Ilic, J., Jansen, S., Lewis, S.L., Miller, R.B., Swenson, N.G., Wiemann, M.C., Chave, J.: Data from: Towards a worldwide wood economics spectrum. Dryad Digital Repository. Dataset (2009). https://doi.org/10.5061/dryad.234 . https://doi.org/10.5061/dryad.234

[45] Thomas, S.C., Martin, A.R.: Carbon content of tree tissues: A synthesis. Forests **3**(2), 332–352 (2012) https://doi.org/10.3390/f3020332

[46] Černý, M.: Biomass of *Picea abies* (L.) karst. in midwestern Bohemia. Scandinavian Journal of Forest Research **5**(1-4), 83–95 (1990) https://doi.org/10.1080/

02827589009382595

[47] Woodland Carbon Code Secretariat / Scottish Forestry: Woodland Carbon Code Version 3.0. Woodland Carbon Code, United Kingdom (2025). Woodland Carbon Code. Accessed: 2026-02-12. https://www.woodlandcarboncode.org.uk/standard/

[48] Jenkins, T.A.R., Mackie, E.D., Matthews, R.W., Miller, G., Randle, T.J., White, M.E.: FC Woodland Carbon Code: Carbon Assessment Protocol (Version 2.0). Forestry Commission, Edinburgh, United Kingdom (2018). Forestry Commission. Accessed: 2026-02-13; 173 pp. https://www.woodlandcarboncode.org.uk/sites/default/files/2025-04/WCC_CarbonAssessmentProtocol_V2.0_March2018.pdf

[49] Mildrexler, D.J., Berner, L.T., Law, B.E., Birdsey, R.A., Moomaw, W.R.: Large trees dominate carbon storage in forests east of the Cascade Crest in the United States Pacific Northwest. Frontiers in Forests and Global Change **3**, 594274 (2020) https://doi.org/10.3389/ffgc.2020.594274

[50] Nolan, V., Gilbert, F., Reed, T., Reader, T.: Distribution models calibrated with independent field data predict two million ancient and veteran trees in England. Ecological Applications **32**(8), 2695 (2022) https://doi.org/10.1002/eap.2695

[51] Dean, C., Kirkpatrick, J.B., Doyle, R.B., Osborn, J., Fitzgerald, N.B., Roxburgh, S.H.: The overlooked soil carbon under large, old trees. Geoderma **376**, 114541 (2020) https://doi.org/10.1016/j.geoderma.2020.114541

[52] Barber, R., Underwood, B., Clarkson, J., Brekke, T., Weeks, T., Wilkinson, T., Wilkes, P., Egan, G., Lee, M., Openshaw, I., Castro, G., Moat, J., Bidartondo, M., Suz, L., Kowal, J.: Ectomycorrhizal community composition and traits predict soil carbon stocks at the landscape scale. Preprint (2025). https://doi.org/10.22541/au.174724213.31661209/v1 . https://doi.org/10.22541/au.174724213.31661209/v1

[53] Lindenmayer, D.B., Laurance, W.F., Franklin, J.F.: Global Decline in Large Old Trees. Science **338**(6112), 1305–1306 (2012) https://doi.org/10.1126/science.1231070

[54] Lindenmayer, D.B.: Conserving large old trees as small natural features. Biological Conservation **211**, 51–59 (2017) https://doi.org/10.1016/j.biocon.2016.11.012

[55] Goodman, R.C., Phillips, O.L., Baker, T.R.: The importance of crown dimensions to improve tropical tree biomass estimates. Ecological Applications **24**(4), 680–698 (2014) https://doi.org/10.1890/13-0070.1

[56] Hunter, F., Ditchburn, B., Burns, N., Strong, C.: NCEA: National trees outside woodland map: Method and user guide report (version 1). Technical report, Forest

Research, Farnham, Surrey, UK (March 2025)

[57] Chavana-Bryant, C., Wilkes, P., Yang, W., Burt, A., Vines, P., Bennett, A.C., Pickavance, G.C., Cooper, D.L.M., Lewis, S.L., Phillips, O.L., Brede, B., Lau, A., Herold, M., McNicol, I.M., Mitchard, E.T.A., Coomes, D.A., Jackson, T.D., Makaga, L., Milamizokou Napo, H.O., Ngomanda, A., Ntie, S., Medjibe, V., Dimbonda, P., Soenens, L., Daelemans, V., Proux, L., Nilus, R., Labrière, N., Jeffery, K., Burslem, D.F.R.P., Clewley, D., Moffat, D., Qie, L., Bartholomeus, H., Vincent, G., Barbier, N., Derroire, G., Abernethy, K., Scipal, K., Disney, M.: ForestScan: A unique multiscale dataset of tropical forest structure across 3 continents including terrestrial, UAV and airborne LiDAR and in-situ forest census data. Earth System Science Data **18**(2), 1243–1274 (2026) https://doi.org/10.5194/essd-18-1243-2026